Rock and Soil Mechanics

Volume 42 | Issue 10 Article 4

1-12-2022

Electrical resistivity evolution of compacted silty clay under drying–wetting cycles sequentially coupled with dynamic loads

Zhi HU
Key Laboratory of Road and Bridge Detection and Maintenance Technology of Zhejiang Province, Zhejiang Scientific Research Institute of Transport, Hangzhou, Zhejiang 310023, China

Pin-bo AI
School of Civil Engineering, Architecture and Environment, Hubei University of Technology, Wuhan, Hubei 430068, China

Zhi-chao LI
China Construction Third Bureau First Engineering Co., Ltd., Wuhan, Hubei 430040, China

Qiang MA
School of Civil Engineering, Architecture and Environment, Hubei University of Technology, Wuhan, Hubei 430068, China

See next page for additional authors

Follow this and additional works at: https://rocksoilmech.researchcommons.org/journal

 Part of the Geotechnical Engineering Commons

Custom Citation

HU Zhi, AI Pin-bo, LI Zhi-chao, MA Qiang, LI Li-hua, . Electrical resistivity evolution of compacted silty clay under drying–wetting cycles sequentially coupled with dynamic loads[J]. Rock and Soil Mechanics, 2021, 42(10): 2722-2732.

This Article is brought to you for free and open access by Rock and Soil Mechanics. It has been accepted for inclusion in Rock and Soil Mechanics by an authorized editor of Rock and Soil Mechanics.

Electrical resistivity evolution of compacted silty clay under drying–wetting cycles sequentially coupled with dynamic loads

Authors

Zhi HU, Pin-bo AI, Zhi-chao LI, Qiang MA, and Li-hua LI

This article is available in Rock and Soil Mechanics: https://rocksoilmech.researchcommons.org/journal/vol42/iss10/4

Rock and Soil Mechanics 2021 42(10): 2722−2732 ISSN 1000−7598
https: //doi.org/10.16285/j.rsm.2021.5443 rocksoilmech.researchcommons.org/journal

Electrical resistivity evolution of compacted silty clay under drying−wetting cycles sequentially coupled with dynamic loads

HU Zhi[1, 2], AI Pin-bo[1], LI Zhi-chao[3], MA Qiang[1], LI Li-hua[1]

1. School of Civil Engineering, Architecture and Environment, Hubei University of Technology, Wuhan, Hubei 430068, China

2. Key Laboratory of Road and Bridge Detection and Maintenance Technology of Zhejiang Province, Zhejiang Scientific Research Institute of Transport, Hangzhou, Zhejiang 310023, China

3. China Construction Third Bureau First Engineering Co., Ltd., Wuhan, Hubei 430040, China

Abstract: The performance evolution of subgrade soil under the coupling effect of drying−wetting cycle and dynamic load is essential for the safety and stability of the subgrade. In this study, a series of electrical resistivity tests was carried out on the compacted silty clay samples subjected to different drying−wetting cycles and dynamic loads using alternating current (AC) two-electrode method. The effect of drying−wetting cycles sequentially coupled with dynamic loads on the electrical resistivity of soil samples was investigated. Then, a mathematical relationship was established to quantitatively characterize the dynamic behaviors of soil samples based on electrical resistivity. Finally, the effectiveness of the electrical resistivity method in evaluating the state of compacted soil was discussed. Test results showed that under the action of drying−wetting cycles coupled with dynamic loads, the electrical resistivity of soil samples decreased greatly with the increases in the number and amplitude of drying−wetting cycles, but the reduction of the electrical resistivity of soil samples caused by dynamic load decreased gradually. The test results can provide a reference for the evaluation of the state of subgrade soil under drying−wetting cycles sequentially coupled with dynamic loads using electrical resistivity method.

Keywords: electrical resistivity; drying−wetting cycle; dynamic load; sequential coupling effect; subgrade soil

1 Introduction

As an essential component of road and railway infrastructure, subgrade directly affects the safety and stability of its operation. In the humid and hot areas of southern China, the subgrade soils are frequently subjected to the combined action of natural climate environment (mainly including the changes of humidity and temperature) and dynamic load of vehicles. The effects of drying−wetting cycles and long-term dynamic load will degrade the subgrade performance, resulting in various subgrade problems such as excessive settlement, uneven deformation and local instability. For this reason, numerous studies have been carried out on the performance evolution of subgrade soil under the single factor effect[1−4] and multi-factor coupling effect[5−9] (e.g. wetting−drying and freezing−thawing cycles, wetting−drying cycle combined with dynamic load, wetting−drying and freezing−thawing cycles combined with dynamic load). During the service period, the performance state of the subgrade soil can be directly obtained by means of field test pit and drilling, but the test procedure is complicated and could damage the subgrade structure to a certain extent. As an alternative, the electrical measurement method can be used to indirectly evaluate the performance state of the subgrade soil, which offers a nondestructive, fast and continuous way for inspecting component[10−11]. The electrical resistivity of soil is influenced by many factors, such as moisture content, soil structure, the property of pore fluid and ambient temperature, which can reflect soil structure and engineering characteristics to a certain extent[12−14]. Bai et al.[15] employed the direct current (DC) two-electrode method to measure the electrical resistivity of compacted residual soil, and revealed that the electrical resistivity of soil samples increased first and then tended to be stable with the increase of the number of drying−wetting cycles. Xiong[16] studied the resistivity characteristics of expansive soil by alternating current (AC) two-electrode method, and found that the electrical resistivity of soil samples gradually decreased and tended to be stable with the increase of the number of drying−wetting cycles. Huang et al.[17] used the DC four-electrode method to measure the electrical resistivity of unsaturated soil, but their results did not present apparent variation trend of electrical resistivity with the increase of the number of drying−wetting cycles. To sum up, there are few studies on the resistivity characteristics of soil under the coupling

Received: 29 March 2021 Revised: 24 June 2021
This work was supported by the National Natural Science Foundation of China (51708190, 52078194).
First author: HU Zhi, male, born in 1989, PhD, Lecturer, mainly engaged in research on engineering properties of unsaturated subgrade soil, subgrade dynamic response. E-mail: huzhi0107@sina.com

effect of drying−wetting cycle and dynamic load in the literature[18−19]. In most of the existing studies, DC power supply was often used. It is easy to produce polarization effect, thus affecting the measurement accuracy[20]. In addition, there is no systematic and in-depth study on the complete evolution process of soil resistivity under the coupled action of drying−wetting cycle and dynamic load. Therefore, it is necessary to carry out further experimental research on soil resistivity characteristics under the coupling effect of drying−wetting cycles and dynamic load.

To this end, a series of cyclic drying and wetting tests and dynamic triaxial tests was carried out on the compacted silty clay under different conditions in this paper. The electrical resistivity of soil samples subjected to the sequential coupling action of drying−wetting cycles and dynamic load under different conditions was measured using AC two-electrode method, and the electrical resistivity evolution of soil samples was obtained. Based on this, the mathematical relationship between electrical resistivity and soil properties was preliminarily established, and the coupling effect on the soil structure and the effectiveness of the electrical resistivity method to evaluate soil state were discussed. The experimental results provide a reference for evaluating the state of subgrade soil under the coupling effect of drying−wetting cycles and dynamic load using electrical resistivity method.

2 Testing program

2.1 Testing materials

The soil samples used in this study were taken from Wuhan, China. The buried depth of the soil is 2−3 m, and the soil is yellowish-brown in color and in a state of hard plastic. The collected soil samples were dried naturally first, and the substances such as stones and plant roots were removed. Next, the samples were crushed by an electric crusher and then passed through the 2 mm sieve. The basic physical properties of the sieved soil sample are listed in Table 1.

Table 1 Indices of basic physical properties of soil samples

Liquid limit /%	Plastic limit /%	Plasticity index	Grain size distribution /%		
			>0.075 mm	0.075−0.005 mm	<0.005 mm
37	20	17	16.1	54.3	29.6

2.2 Sample preparation

Remolded soil samples were used in the test in order to simulate the actual situation of compacted subgrade. In accordance with the requirements of the embankment compaction degree (compaction coefficient $K \geqslant 0.92$) suggested in the '*Code for design of heavy haul railway*' (TB10625−2017)[21], the compaction degree of the soil sample was chosen as 93%, and the dry density was 1.83 g/cm^3. After air drying and crushing, the soil samples were screened with a 0.5 mm sieve, and the pure water was added to prepare the soil samples with an optimum moisture content (OMC) of 16%. Then, soil samples were placed in the desiccator for 24 h. After that, the sample was compacted in three layers to make a cylindrical sample with a diameter of 38 mm and a height of 76 mm, and its actual size and mass were measured. The prepared samples were wrapped with plastic film and stored in a desiccator for later use.

2.3 Cyclic drying and wetting test

In practical engineering, subgrade filling is usually compacted and filled under OMC. Many studies demonstrated that in the natural climate environment, after a period of time, the moisture content of subgrade soil would increase and fluctuate periodically or non-periodically around the equilibrium moisture content (EMC)[22]. Based on this, the path of drying−wetting cycles as shown in Fig.1 was adopted in the test. Firstly, the sample was humidified from OMC to EMC, and then the drying- wetting cycle began. In this study, "EMC−humidification−desiccation−humidification−EMC" is defined as a drying−wetting cycle. The initial moisture content was set the same as OMC of 16%, and the equilibrium water content was set to 17%. The performance of subgrade soil tended to be stable after 4−6 cycles of drying−wetting[3,15,23], thus the maximum number of drying−wetting cycles in the test is six. The amplitudes of drying−wetting cycles are EMC±1%, EMC±3% and EMC±5%.

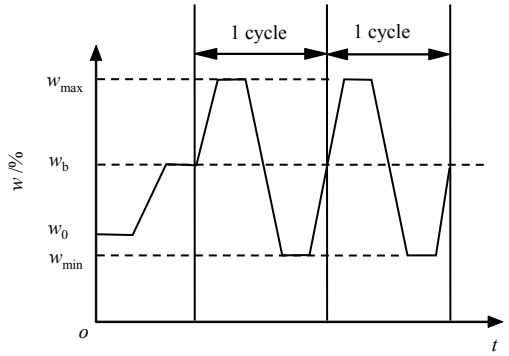

Fig. 1 Schematic diagram of the path of drying−wetting cycles

During the cyclic drying and wetting test, the soil sample was humidified using the humidifier and then air-dried. The moisture content of the sample was indirectly controlled by continuously weighing the sample mass. The device used for the cyclic drying and

wetting test set-up is shown in Fig.2. The prepared samples were put into the humidifier box to increase the moisture content of soil samples. After the samples were humidified to EMC, they were wrapped with plastic film and placed in a desiccator to keep wet for 24 h, in order to homogenize the internal moisture content of the soil samples. When the soil samples reached EMC, maximum or minimum moisture content, they were placed in the desiccator to preserve moisture for 24 h.

Since all the soil samples were in an unsaturated state during the test, matric suction had a significant influence on the mechanical properties of the soil. Due to the negligible differences in the initial volume and compaction degree of soil samples, samples with the same moisture content were regarded as having the same matrix suction in this study. To ensure that the test conditions of the samples were consistent, the moisture content of all soil samples after drying−wetting cycles was strictly controlled at EMC.

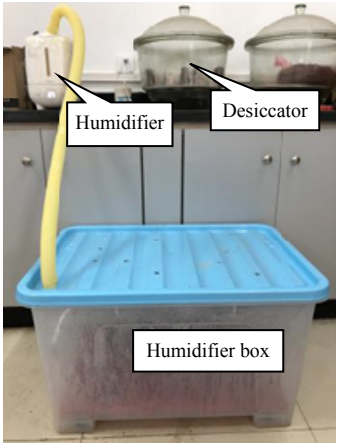

Fig. 2 Cyclic drying and wetting test set-up

2.4 Dynamic triaxial test

The dynamic triaxial tests were carried out using GDS triaxial test system for saturated and unsaturated soils at the Institute of Rock and Soil Mechanics, Chinese Academy of Sciences. The soil samples of 76 mm in height and 38 mm in diameter were used in the test. The dynamic load test adopted the cyclic loading method with stress control, and the loading waveform was half-sine wave. The frequency of train dynamic load is related to train speed, wheelbase and train length, among which the fundamental frequency controlled by train length has the greatest influence on the subgrade[24]. The length L of the existing heavy-haul railway freight carriages in China is 12−15 m[25], and the train speed v is generally not higher than 100 km/h (about 28 m/s). According to $f=v/L$[26], the loading frequency caused by the train is 1.85−2.31 Hz, thus the dynamic loading frequency was set as 2 Hz. The dynamic stress level has a significant effect on the dynamic performance of soil. According to the measured data reported in the literature, the amplitude of dynamic stress in the subgrade soil of heavy-haul railway is about 40−120 kPa, and the average amplitude of dynamic stress in the subgrade soil under 30 t axle load is about 60 kPa[25]. Therefore, the amplitudes of dynamic stress in the test were chosen as 40, 80 and 120 kPa. Before the dynamic load was applied, the samples were consolidated under asymmetrical loading with a confining pressure of 40 kPa, and the consolidation time was set at 12 h. To minimize the change of moisture content of the sample during loading, the pipe valve connected with both ends of the sample was closed in the whole test process, thus isolating the water exchange between the sample and the outside. In this study, the dynamic triaxial test was terminated when the number of loading cycles reached 10 000. The loading process is shown in Fig.3.

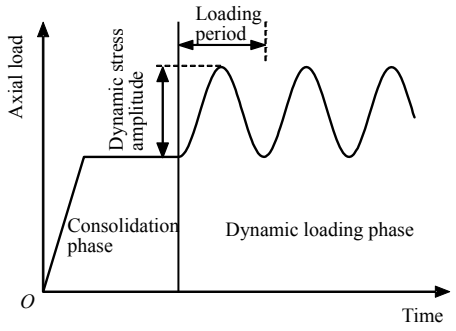

Fig. 3 Schematic diagram of loading process of dynamic triaxial test

At present, there are two methods to consider the coupling effect of various factors on the soil, i.e. direct coupling and sequential coupling[27]. Direct coupling does not consider the iterative action of each factor. While sequential coupling is the iterative coupling analysis of multiple factors, and the results of the previous analysis are applied as the boundary conditions of the subsequent analysis to achieve the research purpose of coupling problems. For the experimental research, it is difficult to achieve the real direct coupling, thus the sequential coupling method is often employed[5−9,18]. Based on this, the test scheme in this study was designed via comprehensively considering the drying−wetting cycle and dynamic load, as listed in Table 2. The soil samples were first subjected to drying−wetting cycles, and then the dynamic load was applied to the samples.

2.5 Electrical resistivity test

The device used in the electrical resistivity test is the TH2817A LCR AC bridge manufactured by Tonghui

Company. The test frequency range provided by this instrument is 50 Hz−100 kHz. To avoid the polarization effect of DC in the process of testing and ensure the integrity of the sample, the AC diode method was used to measure the electrical resistance in the test. Based on previous studies[28−29], the test frequency was selected as 50 kHz and the test voltage was 1 V.

Table 2 Test scheme

Group	Number of drying−wetting cycles	Amplitude of drying−wetting cycle /%	Amplitude of dynamic stress /kPa	Confining pressure /kPa
1	2	0, ±1, ±3, ±5	80	
2	0, 2, 4, 6	±3	80	40
3	2	±3	40, 80, 120	

In the whole process of the drying and wetting cycle, in order to facilitate comparison and accurately reflect the variation of the electrical resistivity of soil samples, 50 g metal block was placed on the surface of the pad electrode sheet above the sample during each measurement. Its purpose was to exert an external contact pressure between the sample and electrode sheet. This ensured that they could fit tightly together and the effect of contact resistance could be minimized (see Fig.4).

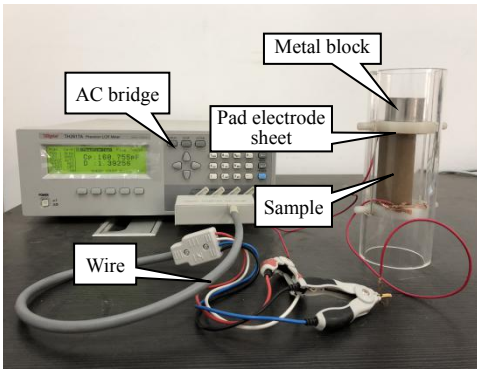

Fig. 4 Apparatus for electrical resistivity testing

The ambient temperature has a significant influence on the results of the electrical resistivity test. Therefore, all the tests in this study were carried out in an air-conditioned room with a constant temperature of 25±1 ℃. However, since the time span from cyclic drying and wetting test to dynamic triaxial test was relatively long, it is found through temperature monitoring that the environmental temperature fluctuated throughout the test. Hence, the temperature correction for electrical resistivity is required. The relationship between the electrical resistivity of the soil ρ_T at different temperatures and that at 25 ℃ is as follows:

$$\rho_T = \frac{\rho_{25}}{1+\alpha(T-25)} \tag{1}$$

where ρ_T and ρ_{25} are the electrical resistivities at temperature T and 25 ℃, respectively; T is the environmental temperature at which resistance is tested; and α is the temperature correction coefficient measured in the test. According to the measured data, α = 0.018 8 ℃$^{-1}$.

3 Test results and discussion

3.1 Dynamic performance of compacted subgrade soil

Figure 5 shows the curves of cumulative plastic strain with the number of vibrations. One of the typical samples in Fig.5 underwent two drying−wetting cycles with amplitude of ±3% and a dynamic stress amplitude of 80 kPa. It can be seen that under different conditions, the cumulative plastic strain of subgrade soil samples increased with the increase of the number of vibrations. However, the cumulative plastic strain of the soil sample that have undergone two drying−wetting cycles was significantly greater than that of the sample without undergoing drying−wetting cycle, increasing by 130% at 10 000 vibrations.

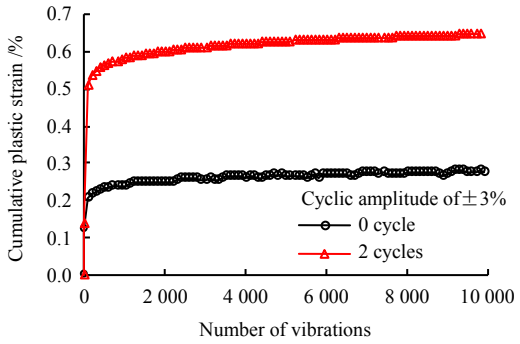

Fig. 5 Evolution curves of cumulative plastic strain of the subgrade soil before and after drying−wetting cycles

Dynamic elastic modulus of soil under dynamic cyclic load represents the ability of the soil to resist deformation. Different from the elastic modulus in the elastic theory, the dynamic elastic modulus is not constant, and it changes as the cyclic load proceeds. In this study, the dynamic elastic modulus of soil is expressed by the slope of the long axis of each load cycle:

$$E_{\mathrm{d}} = \frac{\sigma_{\max} - \sigma_{\min}}{\varepsilon_{\max} - \varepsilon_{\min}} \tag{2}$$

where E_{d} is the dynamic elastic modulus; in a dynamic load cycle, $\sigma_{\max}$ is the maximum dynamic stress; $\sigma_{\min}$ is the minimum dynamic stress; $\varepsilon_{\max}$ is the maximum dynamic strain; and $\varepsilon_{\min}$ is the minimum dynamic strain.

Figure 6 shows the curves of dynamic elastic modulus with the number of vibrations under dynamic cyclic

load. One of the typical samples in Fig.6 underwent two drying−wetting cycles with amplitude of ±3% and a dynamic stress amplitude of 80 kPa. Before 1000 vibrations, the dynamic elastic modulus of the samples showed an increase trend under both test conditions. This suggests that at the initial vibration stage, the cyclic load would increase the dynamic elastic modulus of the sample to a certain extent and improve the sample strength, which might be caused by the compaction of the sample due to vibration. After 1000 vibrations, the dynamic elastic modulus of the sample without drying−wetting cycle increased slowly, while the dynamic model of the sample that has undergone drying−wetting cycle decreased gradually.

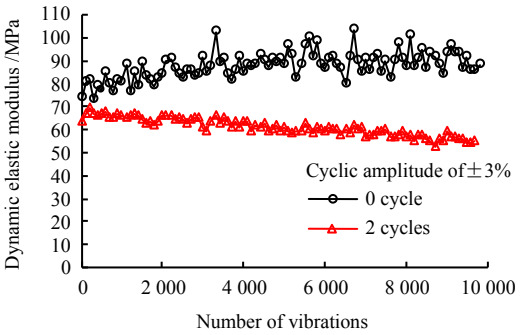

Fig. 6 Evolution curves of dynamic elastic modulus of the subgrade soil before and after drying−wetting cycles

To further study the effect of different conditions of drying−wetting cycle on the dynamic performance parameters of subgrade soil, Table 3 shows the amplitude and variation of the cumulative plastic strain and dynamic elastic modulus of subgrade soil at 10 000 vibrations. It can be seen from Table 3 that the effect of the number of drying−wetting cycles on the dynamic deformation of soil samples was mainly concentrated within 2−4 cycles, which is basically consistent with the effect of the number of drying−wetting cycles on the strength of soil[23]. It is also found that when the amplitude of drying−wetting cycle reached ±5%, the adverse effect on the soil sample became more obvious. When the number of drying−wetting cycles was more than 4, the number of drying−wetting cycles had little effect on the dynamic elastic modulus of the sample. In addition, Table 3 also indicates that the increase of the amplitude of dynamic stress (120 kPa) significantly affected the cumulative plastic strain and dynamic elastic modulus of soil samples.

In conclusion, the drying−wetting cycle has a great influence on the dynamic characteristics of soil samples. Specifically, with the increase of the amplitude or number of wetting drying cycles, the cumulative plastic strain increased, but the dynamic elastic modulus decreased. In the process of drying−wetting cycle, the soil sample experienced volume expansion due to humidification and shrinkage due to water loss during air drying, resulting in the damage of internal structure. On the one hand, the repeated increase and decrease of suction in soil may cause the change of soil structure[1,5,30]. On the other hand, the cemented particles in the soil will dissolve in the water[28−30], producing a large number of microcracks within the soil. With the increase of the amplitude of drying−wetting cycle, the size of the internal cracks within the soil sample also increased, and therefore the deformation became more obvious. Besides, with the increase in the number of drying−wetting cycles, the internal cracks within the sample continued to develop. However, when the number of drying−wetting cycles reached a certain value, the space for the movement of soil particles inside the sample became limited. In the subsequent cycles, the internal cracks of soil had been developed to the limit. Thus the soil particles moved in the existing pores, and the corresponding performance tended to be stable.

Table 3 Variation of dynamic performance of subgrade soil

Number of drying−wetting cycles	Amplitude of drying−wetting cycle /%	Amplitude of dynamic stress /kPa	Cumulative plastic strain /%	Strain amplitude /%	Dynamic elastic modulus /MPa	Amplitude of modulus /%
0	—	80	0.277	—	86.03	—
2	±1	80	0.225	−18.5	87.05	1.2
2	±3	80	0.646	133.6	53.44	−37.9
2	±5	80	0.794	187.2	40.83	−52.5
4	±3	80	0.710	156.8	52.64	−38.8
6	±3	80	0.753	172.3	50.04	−41.8
2	±3	40	0.162	−41.4	70.28	−18.3
2	±3	120	0.851	207.7	41.16	−52.2

3.2 Evolution of electrical resistivity characteristics

3.2.1 Effect of drying and wetting cycle

Figure 7 displays the evolution of the electrical resistivity of the soil sample that has experienced six drying−wetting cycles, in which the amplitude of drying−wetting cycles is ±3%. It can be seen that at EMC, with the increase of the number of drying−wetting cycles, the electrical resistivity of the soil sample gradually decreased and tended to be stable. After six drying−wetting cycles, the electrical resistivity of the sample was reduced by 33% than that without drying−wetting cycles. In a drying−wetting cycle, the electrical resistivity decreased during humidification and increased during air drying. But at the same variation range of moisture content, the change in electrical resistivity caused by air drying process was significantly greater than that caused by humidification process. In general, the electrical resistivity of the sample at the maximum and minimum moisture contents also decreased with the increase of the number of drying−wetting cycles.

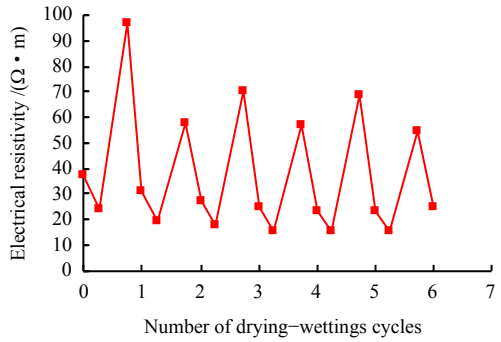

Fig. 7 Evolution of the electrical resistivity of sample under drying−wetting cycles

Due to the technique of sample preparation and the possible inhomogeneity of the sample, the initial electrical resistivity of soil samples under the same test condition might vary slightly. To eliminate the influence of the initial difference of the soil samples on the test results, the electrical resistivity ratio (or normalized electrical resistivity) ρ / ρ_0 was used in this study to analyze the variation of electrical resistivity[31], in which ρ is the electrical resistivity of the sample (Ω • m) and ρ_0 is the initial electrical resistivity of the sample (Ω • m). Here initial electrical resistivity refers to the electrical resistivity measured when the sample reaches EMC for the first time after sample preparation.

Figures 8 and 9 illustrate the effects of different amplitudes and numbers of drying−wetting cycles on the electrical resistivity ratio of the sample, respectively. As seen in Fig.8, the reduction in the electrical resistivity ratio resulting from the drying−wetting cycle with amplitude of ±1% is almost the same as that with amplitude of ±3%. When the amplitude of drying−wetting cycle reached ±5%, the electrical resistivity ratio of the sample decreased more significantly. This indicates that the larger amplitude of drying−wetting cycle has a more obvious effect on soil structure. Similar to the evolution of the electrical resistivity plotted in Fig.7, Fig.9 shows that the electrical resistivity ratio of the sample gradually decreased with the increase of the number of drying−wetting cycles and tended to be stable when the number of cycles was more than 3−4. During the drying−wetting cycle, the pore structure inside the soil sample would change. For cohesive soil, the conductive modes of soil can generally be divided into three types: conductivity of soil particle, conductivity of pore liquid, and conductivity of the combination of soil particle and pore liquid[32]. As the saturation degree of the tested sample with 17% moister content was about 85%−90%, the conductivity of the sample was dominated by the pore fluid, and the conductive modes of the soil particle and the combination of soil particle and pore fluid can be ignored. The drying−wetting cycle will increase the proportion of the macropores and microcracks inside the compacted soil, which is easier to form a through conductive channel for pore liquid. Hence, the electrical resistivity of the sample will be reduced[33]. This effect became more obvious at a larger amplitude of drying−wetting cycle, thus the electrical resistivity decreased more significantly.

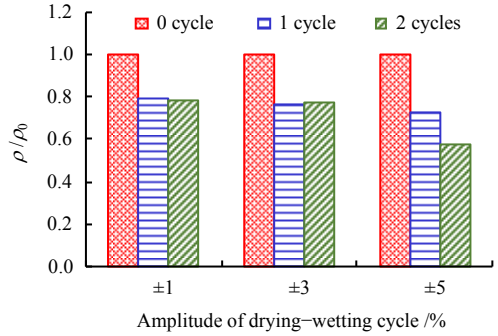

Fig. 8 Effect of the amplitude of drying−wetting cycle on the electrical resistivity of sample

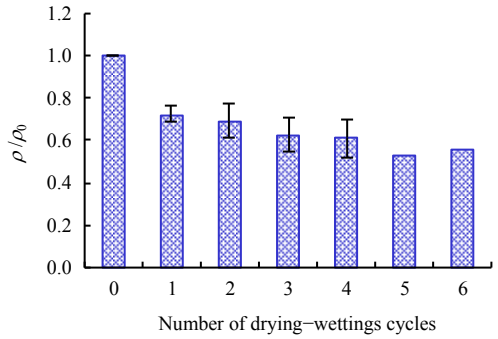

Fig. 9 Effect of the number of drying−wetting cycles on the electrical resistivity of sample

3.2.2 Effect of drying−wetting cycles sequentially coupled with dynamic loads

To explore the effect of drying−wetting cycles sequentially coupled with dynamic loads on electrical resistivity, Figs.10−12 show the effects of the dynamic stress amplitude, and the amplitude and number of drying−wetting cycles on the electrical resistivity ratio of the sample under the coupling action, respectively. Note that the non-cyclic sample in these figures refers to the sample directly subjected to dynamic triaxial test without experiencing drying−wetting cycles, and the dynamic stress amplitude is 80 kPa.

It can be seen from Fig.10 that the dynamic load also led to a decrease in the electrical resistivity ratio of the sample, which decreased by about 25% after experiencing dynamic load. As observed in Table 4, the coupling effect of drying−wetting cycle and dynamic load had little effect on the sample volume, and the sample volume increased less than 0.9%, thus the change in porosity can be ignored. Since dynamic load had a local compaction effect on the sample[5], the sample would rebound when the confining pressure was unloaded after the dynamic triaxial test. The total volume of the sample remained basically unchanged, and the soil sample was also locally compacted. Therefore, the macropores or microcracks inside the sample might

increase compared with those at the end of drying−wetting cycles, and then the connectivity of pore fluid was improved. Meanwhile, the vibration effect could increase the content of dissolved soil particles in pore fluid and the concentration of soluble salt in pore fluid, thus further improving the conductivity of pore fluid[34].

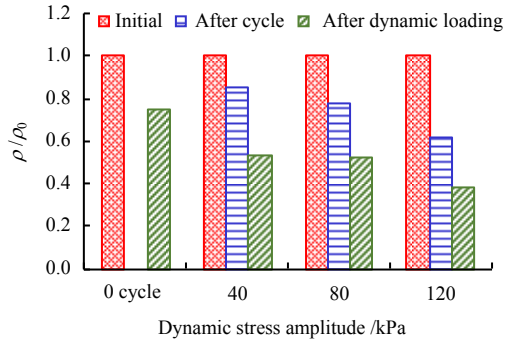

Fig. 10 Effect of dynamic stress amplitude on the electrical resistivity of sample under coupling effect

Table 4 Change in the dimension of samples

Number of drying−wetting cycles	Amplitude of drying−wetting cycle /%	Diameter variation /%	Height variation /%	Volume variation /%	
				After drying−wetting cycles	After vibration
2	±1	0.07	0.10	0.24	0.07
2	±3	0.05	0.09	0.19	0.17
2	±5	0.01	0.88	0.89	0.87
4	±3	−0.04	0.27	0.18	−0.20
6	±3	−0.17	0.42	0.07	0.12

Note: the positive values of diameter, height and volume variations in the table indicate that the size or volume increases, and negative values indicate that the size or volume decreases.

It is also found in Fig.10 that under two drying−wetting cycles with amplitude of ±3%, after the coupling effect, the electrical resistivity ratio of samples decreased with the increase of the dynamic stress amplitude, and the decreasing rate showed an increasing tendency. At the higher dynamic stress amplitude, the electrical resistivity ratio of the sample decreased obviously, indicating that there might be more large pores or microcracks generated inside the soil sample.

One can see from Fig.11 that under the condition of dynamic stress amplitude of 80 kPa and two drying−wetting cycles, the electrical resistivity ratio of the sample under the coupling effect decreased with the increase of the amplitude of drying−wetting cycles. Compared with the cyclic amplitudes of ±1% and ±3%, the reduction in electrical resistivity ratio caused by drying−wetting cycle with amplitude of ±5% was the largest, but the reduction in electrical resistivity ratio caused by dynamic load was the smallest. Therefore, it can be speculated that the new relatively stable soil structure was formed inside the soil sample after the drying−wetting cycles with larger amplitude. For this reason, the effect of dynamic loads on soil structure was weakened with the increase of the amplitude of drying−wetting cycles.

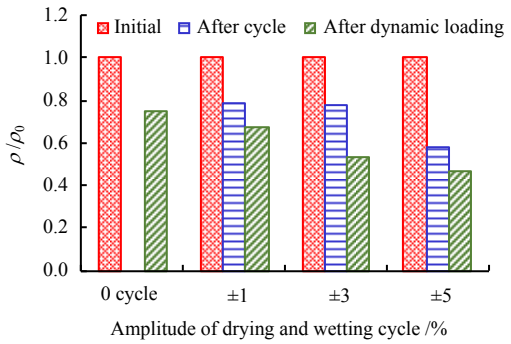

Fig. 11 Effect of the amplitude of drying and wetting cycle on the electrical resistivity of sample under coupling effect

Figure 12 presents that under the conditions of dynamic stress amplitude of 80 kPa and ±3% cyclic amplitude, the electrical resistivity ratio of the sample under the coupling effect decreased with the increase of the number of drying−wetting cycles. Similar to the effect of the amplitude of drying−wetting cycles, the reduction rate of electrical resistivity ratio caused by dynamic loads decreased gradually after more drying−wetting cycles. This is mainly because the development of internal pores in the soil sample was gradually weakened, and the soil structure tended to be relatively stable after several drying−wetting cycles.

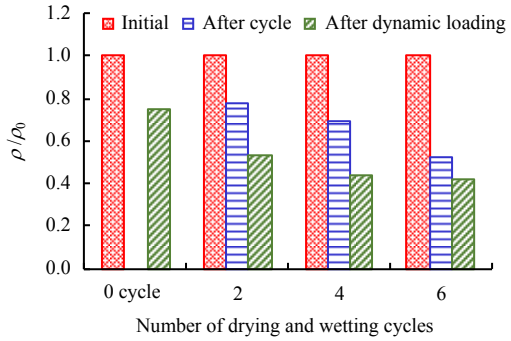

Fig. 12 Effect of the number of drying−wetting cycles on the electrical resistivity of sample under coupling effect

3.3 Quantitative characterization of subgrade soil properties based on electrical resistivity

3.3.1 Correlation between electrical resistivity and mechanical properties

As shown in Fig.13, under the coupling action of drying−wetting cycle and dynamic load, the dynamic elastic modulus and electrical resistivity ratio (ρ / ρ_0) of the subgrade soil decreased exponentially with the number of drying−wetting cycles, while the cumulative plastic strain increased exponentially with the number of drying−wetting cycles. It is particularly emphasized that the electrical resistivity ratio of the sample was obtained after the sample was subjected to 10 000 times of dynamic loading with amplitude of 80 kPa.

In Fig.14, the relationships of dynamic elastic modulus and cumulative plastic strain with electrical resistivity

ratio are linear. Hence, the relationship between the mechanical properties and the electrical resistivity ratio can be established. After that, the measured electrical resistivity ratio can be used to evaluate the mechanical properties of soil indirectly.

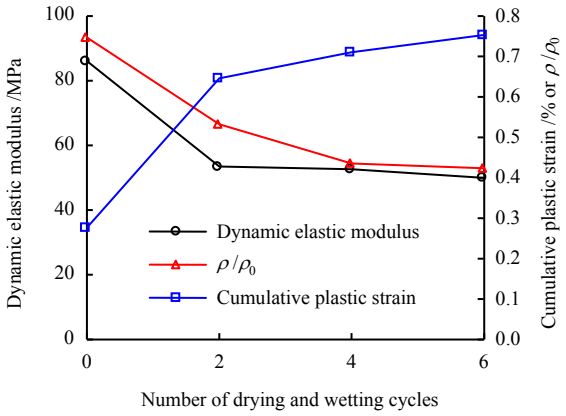

Fig. 13 Variation of dynamic behaviors and electrical resistivity ratio with drying−wetting cycles

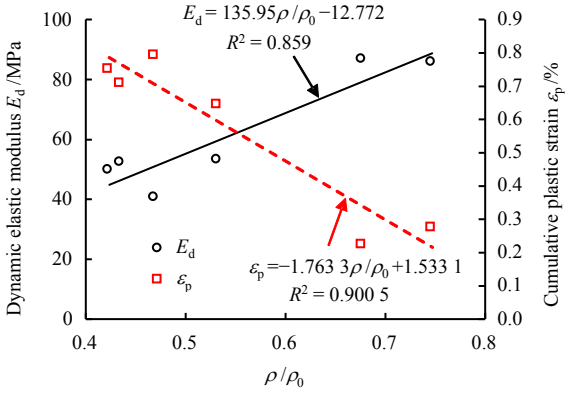

Fig. 14 Relationship between dynamic behaviors and electrical resistivity ratio

3.3.2 Mathematical relationship between drying−wetting cycle and electrical resistivity

Based on the above analysis, it is known that the amplitude of drying−wetting cycles had a linear relationship with the electrical resistivity ratio of the sample (see Fig.8), and the relationship between the number of drying−wetting cycles and the electrical resistivity ratio of the sample was approximately exponential (see Fig.9). Following the relationship between electrical resistivity and the number of drying−wetting cycles proposed by An et al.[35], in this study, it is assumed that there is a mathematical relationship of the electrical resistivity ratio of the sample ρ/ρ_0 with the number of drying−wetting cycles N and the amplitude of drying−wetting cycles R:

$$\frac{\rho}{\rho_0}=a(N^b+c)R+d \tag{3}$$

where a, b, c and d are the fitting parameters.

By performing nonlinear surface fitting on the test data in Figs.8 and 9 based on Eq.(3), the relationship of the electrical resistivity ratio of the sample with the amplitude and number of drying−wetting cycles can be obtained:

$$\frac{\rho}{\rho_0}=-0.073(N^{0.468}-0.131)R+1 \tag{4}$$

When N=0 and R=0, we have ρ/ρ_0=1, which accords with the test result.

This model can describe the evolution of the electrical resistivity ratio of soil samples with the drying−wetting cycles, as shown in Fig.15.

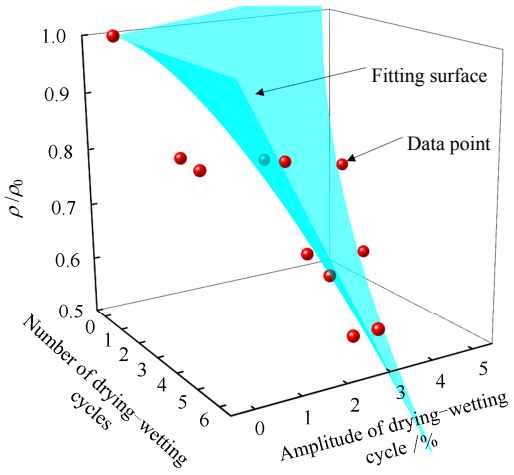

Fig. 15 Evolution of electrical resistivity ratio with drying−wetting cycle

It should be noted that in this study, only three groups of tests considered the effects of different dynamic stress amplitudes, thus the test data obtained are not representative enough and not considered in the model proposed.

3.3.3 Evaluation of soil performance based on electrical resistivity

As shown in Figs.11 and 12, after 10 000 times of dynamic loading with amplitude of 80 kPa, the electrical resistivity ratio ρ/ρ_0 of the sample decreased by 24% on average compared with that of the sample before vibration. The electrical resistivity ratio of the sample before vibration can be obtained using Eq.(4) and the electrical resistivity ratio of the sample after 10 000 times of dynamic loading with amplitude of 80 kPa can be obtained via reducing the results of the sample before vibration by 24%. Then, combined with the relationship given in Fig.13, the dynamic performance of the soil sample can be estimated indirectly.

Figure 16 compares the electrical resistivity ratio and dynamic performance indices of the soil sample obtained using the above method with the measured values. It can be found that on the whole, the fitting curve can well reflect the dynamic elastic modulus and cumulative plastic strain of soil samples with the amplitude and number of drying−wetting cycles. Therefore, it can be preliminarily considered that it is feasible to evaluate the dynamic performance of soil indirectly by electrical resistivity method.

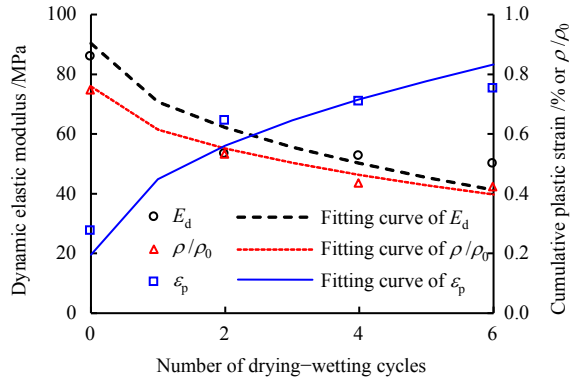

(a) Variation with the number of drying−wetting cycles

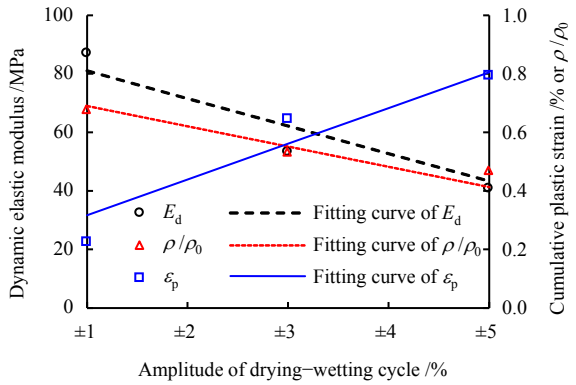

(b) Variation with the amplitude of drying−wetting cycle

Fig. 16 Comparison between estimated and measured values of electrical resistivity and dynamic performance indices

3.4 Discussion

As a nondestructive testing method, the electrical resistivity method is capable of evaluating soil moisture content and mesoscopic structure. However, as the electrical resistivity is affected by many factors such as environmental temperature, humidity and soil structure, most of the evaluations of soil properties using soil resistivity are still qualitative, and it is a great challenge to achieve accurately quantitative evaluation. Therefore, the evaluation method for the properties of subgrade soil based on electrical resistivity is still worthy of further study. The power supply mode of the electrical resistivity test is mainly categorized into two types, i.e. AC power supply and DC power supply. Zhou et al.[20] discussed the two power supply modes and found that the soil sample had a polarization effect under DC voltage, and AC power supply is suitable for the electrical resistivity measurement of soil samples. Specifically, the DC electrical resistivity of soil gradually increased with time, which would result in large errors to the test results. While AC power supply can avoid the polarization effect to the greatest extent and improve the accuracy of test results, but the current frequency has a significant influence on the electrical resistivity of soil samples. In addition, the initial state of soil samples is quite different, and the conductivity characteristics of different types of soils also vary. All of these factors make the application of the electrical resistivity method to soil evaluation become uncertain and insufficiently accurate.

Taking the effect of drying−wetting cycles on the electrical resistivity of soil samples as an example, Fig.17 summarizes the relevant test results published in recent years. The types of soil samples and the drying−wetting cycle conditions in each study (the amplitude of drying−wetting cycles was controlled by mass moisture content) are listed in Table 5. In order to facilitate comparison, the research results are all converted into electrical resistivity ratios ρ/ρ_0. In these existing studies, Bai et al.[15], Lu et al.[18], and Zeng et al.[36] used DC power supply, while Xiong[16], Huang et al.[17] and this study used AC power supply. It can be seen obviously from Fig.17 that the electrical resistivity of the sample with DC power supply increased with the number of drying−wetting cycles, while the results of the test using AC power supply were the opposite. This phenomenon might be related to three factors: (1) the type of soil sample; (2) cyclic drying−wetting paths; and (3) the method of electrical resistivity tests. Firstly, according to the research results, the volume of strongly weathered mudstone and residual soil decreased under the drying−wetting cycle, which inhibited the development of macropores inside the soil sample and gradually weakened the connectivity of conductive channels. However, the volume of silty clay and expansive soil increased under the drying−wetting cycle, and the microcracks and macropores inside the soil were easier to form. Secondly, the strongly weathered mudstone and residual soil experienced the fully saturated state during the drying−wetting cycle, and the suction in the soil approaching zero might lead to the closure of microcracks. In addition, for the unit soil sample, when it reaches saturation, the pore fluid inside the soil sample will be diluted, and the soluble salt concentration of the pore fluid will be reduced. Thus the conductivity of the pore fluid is reduced. However, the maximum moisture contents of silty clay and expansive soil did not reach the saturation degree. The suction in the soil kept the microcracks or macropores open and connected, and the soluble salt inside the soil would not be lost at the same time. Finally, the use of DC may overestimate the electrical resistivity of soil samples due to polarization effect. Direct current has electromotive phenomenon and electrochemical effect, which will change soil moisture content, soil structure, and pore water composition. Meanwhile, DC will also cause polarization effect of electrode and soil, resulting in large errors of electrical resistivity measurement results[20, 37].

In the present study, the initial electrical resistivity was used to normalize the electrical resistivity of the soil sample, and then the evolution of electrical resistivity was obtained. Therefore, the accuracy of the initial electrical resistivity of soil samples is essential in evaluating the performance of subgrade soils. As mentioned above, soil resistivity is affected by moisture

content, compaction degree and pore fluid. When determining the initial electrical resistivity of soil, the interference of some factors such as moisture content should be eliminated as far as possible. Therefore, in practical application, the electrical resistivity can be corrected in combination with the spatial distribution of the moisture content of subgrade soils to obtain a more accurate distribution of initial electrical resistivity.

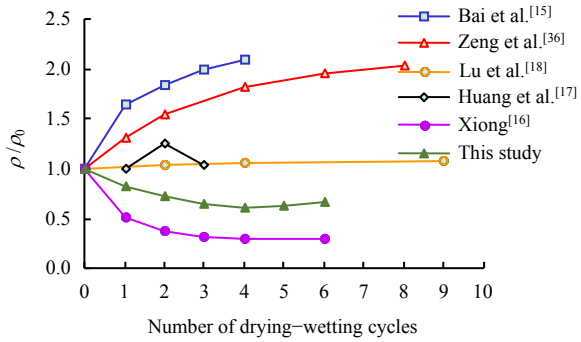

Fig. 17 Comparison of effects of drying−wetting cycles on soil electrical resistivity

Table 5 State of soil sample and conditions of drying−wetting cycle

Source	Dry density /(g • cm^{-3})	Degree of compaction /%	Moisture content /%	Saturation /%	Amplitude of drying−wetting cycle /%	Soil type
Huang et al.[17]	1.65	90.7	25	98.0	5.0−25.0	Clay
Zeng et al.[36]	1.67	—	20	86.0	13.9−saturated	Strongly weathered mudstone
Bai et al.[15]	1.58	95	20	74.3	Air dried−saturated	Residual soil
Lu et al.[18]	1.81	95	17	71.4	15.0−19.0	Silty clay
Xiong [16]	1.55	—	23	85.0	0.0−23.0	Expansive soil
This work	1.83	93	17	85.0	14.0−20.0	Silty clay

Note: In the table, “saturated” means that the saturation degree reaches 100%, and “air dried” means that the water in the soil sample evaporates naturally to a constant mass at room temperature.

To sum up, the electrical resistivity method can effectively reflect the effects of drying−wetting cycles and dynamic loads on soil properties to a large extent, but this method is established based on the evaluation index and approach of actual electrical resistivity. Based on the principle of electrical resistivity test, the quantitative evaluation model of electrical resistivity can be established for different types of soils (such as cohesive soil, sandy soil, soil−rock mixture, and gravel soil), thus forming an evaluation system of subgrade soils based on electrical resistivity method with a strong theoretical background and wide adaptability. In addition, on the premise of fully understanding the evolution of the electrical resistivity of different types of soils, the performance attenuation of subgrade soils can be semi-quantitatively evaluated by further obtaining the spatial distribution of initial electrical resistivity and the electrical resistivity in the service period, thus providing a reference for the performance evaluation and the structural maintenance of subgrade.

4 Conclusions

In this study, based on the evaluation of the performance attenuation and the state of subgrade soils in the service period, the evolution of the electrical resistivity of subgrade soils under drying−wetting cycles sequentially coupled with dynamic loads is studied. The main conclusions are drawn as follows:

(1) With the increases in the number and amplitude of drying−wetting cycles and the dynamic stress amplitude, the cumulative plastic strain increased while the dynamic elastic modulus decreased. The increases of the amplitudes of drying−wetting cycles and dynamic stress had a significant effect on the dynamic performance of the soil sample. The effect of the number of drying−wetting cycles on the dynamic deformation of soil samples was mainly concentrated within 2−4 cycles.

(2) The electrical resistivity of the soil sample decreased with the increases of the amplitude and number of drying−wetting cycles and became stable after 3−4 cycles. The electrical resistivity of compacted clay decreased under the dynamic loading. With the increase of the dynamic stress amplitude, the decreasing rate of electrical resistivity showed an increasing trend.

(3) Under drying and wetting cycles sequentially coupled with dynamic loads, with the increases of the number and amplitude of drying−wetting cycles, the electrical resistivity of compacted soil samples decreased, but the reduction in electrical resistivity caused by dynamic loading gradually decreased.

(4) The relationships of dynamic elastic modulus and cumulative plastic strain with electrical resistivity ratio are linear. The electrical resistivity test can well reflect the effect of drying−wetting cycles on soil properties, but it is necessary to establish the corresponding electrical resistivity evaluation models for different types of soils.

References

[1] ZHANG Jun-ran, XU Qiang, SUN De-an. Simulation of soil-water characteristic curves during drying and wetting cycles[J]. Rock and Soil Mechanics, 2014, 35(3): 689−695.

[2] LÜ Meng-fei, CHEN Kai-sheng. Influence of red clay elastic modulus on pavement structure under drying−wetting cycles[J]. Journal of Guangxi University (Natural Science Edition), 2018, 43(4): 1618−1624.

[3] XIE Hui-hui, XU Zhen-hao, LIU Qing-bing, et al. Evolution of peak strength and residual strength of weak expansive soil under drying-wetting cycle paths[J]. Rock and Soil Mechanics, 2019, 40(Suppl. 1): 245−252.

[4] CHEN Yong, ZHAO Qiang, CHAN D. Impact and prediction of wetting-drying cycles on seismic response of silty clay[J]. Journal of China Three Gorges University (Natural Sciences), 2017, 39(6): 52−56.

[5] LIU Wen-hua, YANG Qing, TANG Xiao-wei, et al. Experimental study on the dynamic characteristics of unsaturated soils under traffic loading[J]. Journal of

Disaster Prevention and Mitigation Engineering, 2015, 35(2): 263−269.

[6] MO Wen-yu. Experimental study on the dynamic properties of lime-treated expansive soil affected by wetting-drying cycles[D]. Nanning: Guangxi University, 2015.

[7] LI Xing, CHENG Qian-gong, ZHANG Jin-cun, et al. Experimental study on dynamic performance of cement-improved expansive soil in high speed railway subgrade in wetting-drying cycles[J]. Railway Engineering, 2016(6): 99−103.

[8] ZENG Zhi-xiong, KONG Ling-wei, LI Jing-jing, et al. Mechanical properties and normalized stress-strain behaviour of Yanji swelling rock under wetting-drying-freezing-thawing cycles[J]. Rock and Soil Mechanics, 2018, 39(8): 2895−2904.

[9] WANG Fei, YANG Bao-cun. Experimental study on the deformation of the stable layer of road water under the sequential coupling effect of drying-wetting and freezing-thawing and vehicle load[J]. Science Technology and Engineering, 2018, 18(29): 232−238.

[10] YUAN G, CHE A, FENG S. Evaluation method for the physical parameter evolutions of highway subgrade soil using electrical measurements[J]. Construction and Building Materials, 2020, 231: 117162.

[11] LI Rui-ke, CHE Ai-lan, FENG Shao-kong. Electrical measurement based laboratory testing method of physical properties of subgrade soil[J]. Journal of Engineering Geology, 2020, 28(1): 51−59.

[12] ZHA Fu-sheng, LIU Jing-jing, XU Long, et al. Electrical resistivity of heavy metal contaminated soils solidified/ stabilized with cement-fly ash[J]. Rock and Soil Mechanics, 2019, 40(12): 4573−4580, 4606.

[13] XU Lei. Study on engineering properties of expansive soil by resistivity in situ test[D]. Nanjing: Southeast University, 2017.

[14] SONG Jie, LI Shu-cai, LIU Bin, et al. Quantitative assessment method of unsaturated soil compaction degree based on resistivity property[J]. Journal of Chang'an University (Natural Science Edition), 2015, 35(6): 33−41.

[15] BAI W, KONG L, GUO A. Effects of physical properties on electrical conductivity of compacted lateritic soil[J]. Journal of Rock Mechanics and Geotechnical Engineering, 2013, 5(5): 406−411.

[16] XIONG Fu-cai. Study on the mechanical properties of the resistivity of Hefei expansive soil[D]. Hefei: Hefei University of Technology, 2016.

[17] HUANG C, HUGHES P, TOLL D, et al. Electrical resistivity and mechanical behaviour of unsaturated soil under multiple cycles of drying and wetting[C]//7th International Conference on Unsaturated Soils 2018. Hong Kong: [s. n.], 2018.

[18] LU Z, WU X, HU Z, et al. Electric resistance tests on compacted clay material under dynamic load coupled with dry-wet cycling[J]. Advances in Materials Science and Engineering, 2018(6): 1−6.

[19] WANG Zhi-peng. Soil resistivity testing and its application in dynamic slaking test[D]. Shijiazhuang: Shijiazhuang Tiedao University, 2016.

[20] ZHOU Mi, WANG Jian-guo, HUANG Song-bo, et al. Experimental investigation on influencing factors in soil resistivity measurement[J]. Rock and Soil Mechanics, 2011, 32(11): 3269−3275.

[21] The Third Railway Survey and Design Institute Group Corporation. TB 10625—2017 Code for design of heavy haul railway[S]. Beijing: China Railway Publishing House, 2017.

[22] HU Zhi. Research on performance deterioration of subgrade under high-speed train load coupled with drying-wetting cycles[D]. Beijing: University of Chinese Academy of Sciences, 2016.

[23] LÜ Hai-bo, ZENG Zhao-tian, ZHAO Yan-lin, et al. Experimental studies of strength of expansive soil in drying and wetting cycle[J]. Rock and Soil Mechanics, 2009, 30(12): 3797−3802.

[24] ZHAO Ming-long. The effect of cyclic dry-wet process on the dynamic behavior of cement-soil[D]. Tianjin: Tianjin University, 2005.

[25] JIA Jin-zhong. Dynamic load characteristic of heavy haul railway subgrade[J]. Railway Engineering, 2014(7): 89−91.

[26] GONG Quan-mei, LUO Zhe, YUAN Jian-yi. Experimental study on long-term cumulative settlement and equivalent cyclic load of speed-up railway subgrade soil[J]. Journal of the China Railway Society, 2009, 31(2): 88−93.

[27] YAN Bing-qian, REN Fen-hua, CAI Mei-feng, et al. A review of the research on physical and mechanical properties and constitutive model of rock under THMC multi-field coupling[J]. Chinese Journal of Engineering, 2020, 42(11): 1389−1399.

[28] HU Z, PENG K, LI L, et al. Effect of wetting-drying cycles on mechanical behaviour and electrical resistivity of unsaturated subgrade soil[J]. Advances in Civil Engineering, 2019(12): 3465327.

[29] LI Zhi-chao. Dynamic characteristics and meso-damage evolution of subgrade soil under dry-wet cycle[D]. Wuhan: Hubei University of Technology, 2020.

[30] TANG C S, WANG D Y, ZHU C, et al. Characterizing drying-induced clayey soil desiccation cracking process using electrical resistivity method[J]. Applied Clay Science, 2018, 152: 101−112.

[31] WU G, WANG K, ZHAO M, et al. Analysis of damage evolution of sandstone under uniaxial loading and unloading conditions based on resistivity characteristics[J]. Advances in Civil Engineering, 2019(2): 9286819.

[32] ZHA Fu-sheng, LIU Song-yu, DU Yan-jun, et al. The electrical resistivity characteristics of unsaturated clayey soil[J]. Rock and Soil Mechanics, 2007, 28(8): 1671−1676.

[33] WANG D Y, TANG C S, CUI Y J, et al. Effects of wetting-drying cycles on soil strength profile of a silty clay in micro-penetrometer tests[J]. Engineering Geology, 2016, 206: 60−70.

[34] MA De-cui. Research on dynamic response to vibratory loads of silty soils and the physical mechanics in the Yellow River estuary[D]. Qingdao: Ocean University of China, 2005.

[35] AN Ran, KONG Ling-wei, BAI Wei, et al. The resistivity damage model of residual soil under uniaxial load and the law of drying-wetting effects[J]. Chinese Journal of Rock Mechanics and Engineering, 2020, 39(Suppl.1): 3159−3167.

[36] ZENG Z X, KONG L W, WANG M, et al. Assessment of engineering behaviour of an intensely weathered swelling mudstone under full range of seasonal variation and the relationships among measured parameters[J]. Canadian Geotechnical Journal, 2018, 55(12): 1837−1849.

[37] LIU Song-yu, ZHA Fu-sheng, YU Xiao-jun. Laboratory measurement techniques of the electrical resistivity of soils[J]. Journal of Engineering Geology, 2006, 14(2): 216−222.